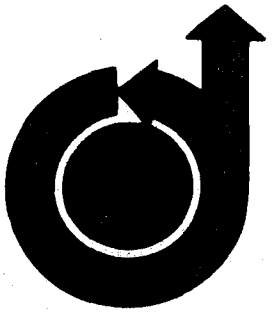

AIAA Paper No. 74-201

COMPARISON OF APPROXIMATE AND NUMERICAL ANALYSES OF NONLINEAR COMBUSTION INSTABILITY

by
F. E. C. CULICK
California Institute of Technology
Pasadena, California
and
J. N. LEVINE
Ultrasystems, Incorporated
Irvine, California

AIAA 12th Aerospace Sciences Meeting

WASHINGTON, D.C. / JANUARY 30-FEBRUARY 1, 1974

COMPARISON OF APPROXIMATE AND NUMERICAL ANALYSES OF NONLINEAR COMBUSTION INSTABILITY

F. E. C. Culick
California Institute of Technology
Pasadena, California

J. N. Levine
Ultrasystems, Inc.
Irvine, California

Abstract

At the present time, there are three general analytical techniques available to study problems of unsteady motions in rocket motors: linear stability analysis; approximate nonlinear analysis, founded on examining the behavior of coupled normal modes; and numerical calculations based on the conservation equations for one-dimensional flows. The last two yield the linear results as a limit. It is the main purpose of this paper to check the accuracy of the approximate analysis against the numerical analysis for some special cases. The results provide some justification for using the approximate analysis to study three-dimensional problems.

I. Introduction

When unstable pressure oscillations occur in a combustion chamber, the most important practical consideration is the amplitude of the motions. Because the combination of the combustion processes and the flow field is a self-excited system - no external influences are involved - an unstable motion will reach a limiting amplitude only through the action of one or more nonlinear processes. The general character of the unsteady motion is that initially a small amplitude disturbance in the flow is intrinsically unstable and is therefore amplified. Interactions between the disturbance and the combustion processes provide the necessary transfer of energy to sustain the motion. Eventually, either those interactions or some other process, such as a loss of energy due to viscous forces, become nonlinear and the time-averaged flow of energy to the disturbance is reduced to zero. Formally, the system executes a limit cycle. There are conditions, neither well-defined nor understood, when small disturbances may be stable, but the system may be unstable to a large disturbance which develops into a limit cycle.

Most of the published works on problems of combustion instability in solid propellant rocket motors have been concerned with the relatively simpler question of linear stability for small disturbances (e. g. refs. 1-5). Those linear analyses provide no information about the limiting amplitudes. Recently, considerably more emphasis has been placed on nonlinear behavior. Both numerical calculations (refs. 6-9) and approximate analyses (refs. 10, 11) have been reported. The purpose of this paper is to describe the two ways of analyzing the problem and to compare some results.

There are necessarily some assumptions and approximations required to define the problem. Numerical solutions to the differential equations, and whatever boundary conditions are used, then constitute the closest one can approach an "exact" solution. The point of view taken here, therefore, is that the numerical solutions must in some sense be used to check the results of an approximate analysis. For reasons which will be clear later, this is not quite so straightforward as one would like. At the present time, the limitations imposed separately on the two approaches, but particularly on the approximate analysis, are such that only a few special cases can be examined. Moreover, the results are not immediately comparable in all respects. The principal difference is that the numerical solution gives the complete pressure and velocity waveforms, while the approximate analysis gives the time-dependent behavior of a finite number of harmonic components of the waves.

The primary simplification used in the existing numerical analyses is that fluid motion is limited to one dimension. Consequently, only longitudinal motions can be treated, which means that motors having, for example, slots and fins, or exhibiting tangential instabilities, cannot be analyzed. The approximate analysis can be used with comparable ease (or difficulty) for all geometries. For the purposes here, both approaches are based on the same set of differential equations. However, the influence of both the exhaust nozzle and the combustion processes, which enter as boundary conditions, are more accurately accounted for in the numerical analysis.

For practical purposes, one would like eventually to devise a relatively simple and inexpensive means of calculating both the stability and limiting amplitude of a disturbance. An approximate analysis is more likely to be successful in this respect. However, there are many features of nonlinear behavior which can be studied in detail only with "exact" numerical solutions. It is not the purpose here to cover thoroughly the numerical results which have been obtained (refs. 6-9), and which have been very useful. We wish mainly to describe the connections between the two approaches and to examine a few results. Examples given include problems of transient wave motion in a box containing a gas/particle mixture (no combustion or flow) and some cases of instability in small laboratory motors. In view of the simplifications introduced in the approximate analysis, the agreement is surprisingly good, although not wholly satisfactory.

II. The One-Dimensional Problem

The equations for one-dimensional unsteady flow in a solid propellant rocket motor have been amply discussed in previous works (e. g. refs. 4 and 6). For simplicity, only motions in uniform chambers will be discussed. Because solid propellants which contain metal will produce condensed material in the combustion products, the equations of motion must be written for a two-phase flow. Residual combustion, condensation, and coalescing of particles within the volume will be ignored. Thus, it is assumed that inert parti-

cles are produced in the very thin combustion zone at the burning surface, leave in the direction normal to the surface, and join the flow with no further changes in their physical properties. Moreover, it is assumed that the behavior of the particulate matter may be described by a single average size, and single local values of temperature and speed. The complete set of equations for the two-phase flow field are:

mass

gas $$\frac{\partial \rho}{\partial t} + \frac{\partial}{\partial z}(\rho u) = \alpha \qquad (2.1)$$

particles $$\frac{\partial \rho_p}{\partial t} + \frac{\partial}{\partial z}(\rho_p u_p) = \beta\alpha \qquad (2.2)$$

momentum

gas $$\frac{\partial(\rho u)}{\partial t} + \frac{\partial}{\partial z}(\rho u^2 + p) = F_p - \beta\alpha u_p \qquad (2.3)$$

particles $$\rho_p \frac{\partial u_p}{\partial t} + \rho_p u_p \frac{\partial u_p}{\partial z} = -F_p \qquad (2.4)$$

energy

gas $$\frac{\partial(\rho e_o)}{\partial t} + \frac{\partial}{\partial z}(\rho u e_o) + \frac{\partial}{\partial z}(up) =$$
$$\alpha h_{so} + Q_p + u_p F_p + \beta\alpha(e_{pos} - e_{po}) \qquad (2.5)$$

particles $$\rho_p \frac{\partial e_p}{\partial t} + \rho_p u_p \frac{\partial e_p}{\partial t} = -Q_p \qquad (2.6)$$

The gas phase is treated as a single (average) species obeying the equation of state for a perfect gas:

$$p = \rho R T \ . \qquad (2.7)$$

Erosive burning will be ignored, and the linear regression rate of the propellant material is represented by

$$r = c p^n \ , \qquad (2.8)$$

where c, n are constant. The total mass flux of material leaving the burning surface is therefore $\rho_s r$. Hence, the total rate (i.e., gas and particulate matter) entering the chamber per unit length is $\rho_s r q$, where q is the perimeter. The quantities α and β are so defined [see (2.1) and (2.2)] that with S_c the cross-section area of the channel, αS_c and $\beta\alpha S_c$ are the rates at which gas and particles are added to the flow, per unit length. Thus, the sum of αS_c and $\beta\alpha S_c$ equals $\rho_s r q$, and the source function is

$$\alpha = \rho_s r \frac{q}{S_c(1+\beta)} \ . \qquad (2.9)$$

Exchange of momentum and energy between the gas and particulate matter occurs through the action of the force F_p and the heat transfer Q_p. Nonlinear representations are easily handled in the numerical analysis; for example, in refs. 6, 7, the following forms are used:

$$F_p = \frac{18\mu}{\rho_s \sigma^2} \rho_p (u_p - u)\left[1 + \frac{1}{6} Re^{2/3}\right] \qquad (2.10)$$

$$Q_p = \frac{6 C_p \mu}{\rho_s Pr \sigma^2} \rho_p (T_p - T)\left[2 + .459 Re^{.55} Pr^{.33}\right] \qquad (2.11)$$

where the Reynolds number is based on the relative flow speed:

$$Re = \frac{\rho\sigma}{\mu} |u_p - u| \ . \qquad (2.12)$$

The force (2.10) is based on the drag coefficient for a single sphere in steady flow (ref. 12). The heat transfer is based on the expression given in ref. 13 for the Nusselt number in steady flow. At present only linear expressions are used in the approximate analysis. Those are found by setting Re = 0 in (2.11) and (2.12).

For the problems discussed here, the head end (z = 0) of the chamber is assumed to be inert and rigid. Thus, the velocity of the gas and particles is zero there. The boundary condition at the aft end of a motor is specified somewhat differently for the two kinds of calculations. In the approximate analysis, the exhaust nozzle is most conveniently analyzed as a separate problem; its influence on wave motions in the chamber is incorporated as a boundary condition set at z = L, by definition the end of the chamber. The boundary condition is concisely and conveniently expressed in terms of an admittance function. A very simple result for short nozzles, based on the assumption of isentropic quasi-steady flow, is used in this work.

In the numerical analyses, the influence of the exhaust nozzle can be treated in several ways. The representation used in the approximate analysis can also be accommodated by the numerical analysis. A better approximation, still for quasi-steady flow, can be obtained by using a "fractional-lag" analysis for the nozzle (refs. 6, 14). The most accurate treatment within the approximation of one-dimensional flow is obtained by solving the general conservation equations in the convergent section of the nozzle and through the throat into the supersonic region (refs. 7-9).

The most difficult and least certain part of the entire problem, no matter what kind of analysis is used for the fluid mechanics, is the boundary condition along the burning surface. What is required is a specification of the change of mass flux leaving the surface in response to a change of pressure. It has been established beyond doubt, by both experimental and theoretical work, that the process can not be accurately represented by the quasi-steady approximation except for rates of change very much slower than those associated with acoustic waves. For small-amplitude, steady harmonic oscillations of pressure, the boundary condition on the mass flux can be written in terms of a response function R_b,

$$\frac{m'}{\bar{m}} = R_b \frac{p'}{\bar{p}} \ . \qquad (2.13)$$

Most analyses of the problem (ref. 15) lead to a simple formula for the response function,

$$R_b = \frac{nAB}{\lambda + \frac{A}{\lambda} - (A+1) + AB} \qquad (2.14)$$

where A and B are parameters related to the combustion of the propellant in steady state, and λ is a complex function of frequency.

For an arbitrary disturbance p'(t), (2.14) can be used as an inverse transform to give m'(t). There are some practical difficulties which have been resolved in the numerical analysis (ref. 6). However, under many circumstances, a nonlinear

computation should be used (refs. 7-9). At the present time, the approximate analysis does not include either the truly transient character of the response or nonlinear behavior. This is a potentially serious weakness which has not yet been fully assessed.

In the numerical analyses, the set of equations (2.1) - (2.9), as shown or in slightly different forms, have been solved by finite difference techniques, and/or by the method of characteristics. These equations constitute the starting point of the approximate analysis outlined in §4. It is the purpose of the work discussed here to provide an initial assessment of the additional assumptions introduced in the approximate analysis.

III. Numerical Analysis

Broadly, there are three main parts to the numerical analysis: the solution for the steady flow, the solution for the transient motions within the volume, and computations associated with the boundary conditions presented by the nozzle and the burning surface. In ref. 6, the steady-state solution within the chamber was determined by solving the equations for steady-state two-phase flow written explicitly in the form of conservation equations. The result was matched to numerical solution for quasi-steady flow in the nozzle based on the fractional lag approximation (ref. 11).

The method of characteristics was used in ref. 6 to compute the transient motions. It is necessary then to write the equations in a more suitable form than given in §2, and in addition there are a considerable number of computational details which will not be included here. A crucial part of the problem, quite apart from the numerical analysis of the motions within the chamber, is the treatment of the transient burning response.

Difficulties arise because the transient mass flux due to changes in the burning rate leads or lags changes in the chamber pressure. The time lag (or lead) is, in general, comparable to a typical period of oscillation in the chamber pressure. Consequently, the burning rate at a particular instant of time depends on the past history of the chamber pressure. In ref. 6, a method was worked out for handling this problem based on the inverse transform of eq. (2.14). The results were therefore limited, strictly, to small (linear) changes of burning rate.

The calculations reported in ref. 7 incorporate some important changes. These not only reduce substantially the computing costs, but also increase the flexibility of the analysis: many more special problems can be accommodated. The most significant changes are that the computations within the volume of the chamber are done with a finite difference method (ref. 13); and the calculation of the transient burning rate accounts for nonlinear behavior. The numerical calculations reported in refs. 8, 9 are based on similar techniques.

IV. Approximate Analysis

The approximate analysis used here (ref. 11) is based on expansion of the unsteady pressure and velocity fields in the natural modes of the chamber. More details will be given here than for the numerical analysis so that the approximations involved may be more clearly shown. If p', $\vec{u}'$ denote the deviations of pressure and velocity from the mean values, then these are assumed to have the forms

$$p' = \bar{p} \Sigma \eta_n(t) \psi_n(\vec{r}) , \qquad (4.1)$$

$$\vec{u}' = \Sigma \frac{\dot{\eta}_n(t)}{\bar{\gamma} k_n^2} \nabla \psi_n . \qquad (4.2)$$

Here, $\bar{\gamma}$ and other properties, including the speed of sound, are values for equilibrium behavior of the gas/particle mixture. That these are the correct values to use has been shown in ref. 5. The $\psi_n(\vec{r})$ are the classical normal modes for a closed chamber having the same geometry as the rocket motor and the $\eta_n(t)$ are functions of time to be determined. Eventually, the problem is reduced to solving a set of coupled nonlinear equations for the $\eta_n(t)$. Interpretation of the general formulation of the problem is immediately clear from the equations: the pressure field is represented as an infinite set of coupled harmonic oscillators, having the amplitudes $\eta_n(t)$. There is one oscillator for each natural mode or harmonic of the chamber. Several approximations are required to produce this representation; but in order to obtain solutions, the most serious influence on the numerical results may be the necessity to cut off the series (4.1) and (4.2) so that the field is represented by a finite number of oscillators.

There are experimental results suggesting that the unstable motions in motors may sometimes consist only of a small number of harmonics. Indeed, the first attempt (ref. 10) to analyze the problem in this way used the assumption that the pressure field could be approximated by a single natural mode. For example, records of firings in T-burners, and some motors as well, appear to be cleanly sinusoidal with slowly varying amplitude and frequency. However, harmonic analysis of such records has shown that in fact there may be significant content of higher harmonics; and there are many records showing quite obviously that higher harmonics are excited. The analysis was therefore extended in ref. 11 to accommodate all modes of the chamber.

The analysis may be conveniently divided into five parts:

(i) expansion of the pressure and velocity fields in two small parameters, a characteristic Mach number of the steady flow field and the amplitude (or Mach number) of the disturbance;

(ii) construction of a nonlinear wave equation with boundary conditions, for the unsteady pressure field;

(iii) substitution of the expansions (4.1) and (4.2), and formation of the nonlinear ordinary differential equations for the $\eta_n(t)$;

(iv) reduction of the second order equations for the $\eta_n(t)$ to first order equations by making use of the observed feature that the amplitudes and frequencies (or phases) of the $\eta_n(t)$ are slowly varying in time;

(v) numerical solution of the first order equations.

A considerable amount of arithmetic is required in steps (i) - (iii). The equations for the η_i, obtained from integration of the partial differential equations over the volume of the chamber, have the form

$$\ddot{\eta}_n + \omega_n^2 \eta_n = F_n \ . \qquad (4.3)$$

The "force" F_n acting on the n^{th} oscillator is, in general, a nonlinear function of both the displacements η_i and the velocities $\dot{\eta}_i$ of all the oscillators. To the present time, only nonlinearities associated with the fluid mechanics within the volume have been accounted for. The influences of the particles, combustion processes, and the exhaust nozzle are all represented by linear approximations. There is no obstacle in principle, but the details of working out the nonlinear representations are difficult. Moreover, the acoustical nonlinearities have been carried out only to second order. Under these conditions, the function F_n has the form

$$F_n = -\sum_{i=0}^{\infty} [D_{ni}\dot{\eta}_i + E_{ni}\eta_i] + \iint \psi_n \frac{\partial R}{\partial t}\, dS$$
$$- \sum_{i=0}^{\infty}\sum_{j=0}^{\infty} [A_{nij}\dot{\eta}_i\dot{\eta}_j + B_{nij}\eta_i\eta_j] \ . \qquad (4.4)$$

The surface integral in (4.4) represents the influence of combustion; for the problems discussed here, the quantity R is related to the fluctuation of mass flux leaving the surface by

$$R(t) = \frac{\bar{\gamma}(1+\varkappa)}{E_n^2} \frac{m'(t)}{\bar{\rho}} \ , \qquad (4.5)$$

where $\bar{\rho}$ is the average density of the mixture and $\varkappa$ is the ratio of the mass of condensed material to the mass of gas in a unit volume of chamber. Strictly, as the remarks in §§ 2 and 3 have indicated, the truly transient behavior of the combustion response should be accounted for. Although the numerical calculation of m'(t) for an arbitrary pressure disturbance can be handled, using the method developed in ref. 6, a simpler approximation is used here. It is assumed that the intrinsic transient behavior of the combustion dies out so quickly that the long time frequency response can be used. Thus, m' in (4.5) must in some sense be proportional to the response function defined in (2.13). Now the response function is a complex function of frequency, and because for harmonic motions $d/dt = i\omega$, equation (2.13) can be written

$$\frac{m'}{\bar{m}} = [R_b^{(r)} + iR_b^{(i)}]\frac{p'}{\bar{p}} = R_b^{(r)}\frac{p'}{\bar{p}} + \frac{1}{\omega} R_b^{(i)} \frac{d}{dt}\left(\frac{p'}{\bar{p}}\right) \ . \qquad (4.6)$$

The assumption is that (4.6) may be used in the surface integral appearing in (4.4) for any pressure field. When the expansion (4.1) is then substituted, only a single term remains in the n^{th} equation, namely that corresponding to η_n. The terms are therefore proportional to the real or imaginary parts of R_b, evaluated at the frequency ω_n.

Consequently, the combustion term in (4.5) contributes to D_{nn} and E_{nn} only. It will be shown shortly that D_{nn} is twice the growth, or decay, constant for the n^{th} mode, and that the terms D_{ni}, E_{ni} for $i \neq n$ do not influence the approximate solutions to (4.5) when longitudinal modes are considered. Thus, the linear terms produce no coupling between modes. This result appears to be inconsistent with the familiar phenomenon of beating found, for example, when two simple pendula are coupled. The difference is that for the longitudinal modes, the frequencies are integral multiples of the fundamental frequency; to obtain beating, the frequencies of two oscillators should be close, and not in the ratio of whole numbers.

Although the coupled set of equations (4.5) can be solved numerically, it is entirely consistent with the approximations used in simplifying the original partial differential equations, and also considerably less expensive, to reduce them to first order equations before carrying out numerical solutions. This may be accomplished either by the technique based on expansion in two time variables (ref. 16) or by application of the method of averaging (ref. 17). For the general problem, both methods require extension, and at the present time, it appears that only with the method of averaging can one treat cases in which the frequencies are not integral multiples of the fundamental.

In either case, one assumes first that the amplitudes $\eta_n(t)$ can be expressed in the form

$$\eta_n(t) = A_n(t)\sin\omega_n t + B_n(t)\cos\omega_n t \ , \qquad (4.7)$$

where A_n, B_n are slowly varying functions of time in the sense that fractional changes are small during one period. By a relatively simple argument (ref. 11), which will not be reproduced here, the A_n, B_n must be found from the first order equations

$$\frac{dA_n}{dt} = \frac{1}{2\pi}\int_0^{2\pi/\omega_n} F_n \cos\omega_n t'\, dt' \qquad (4.8)$$

$$\frac{dB_n}{dt} = -\frac{1}{2\pi}\int_0^{2\pi/\omega_n} F_n \sin\omega_n t'\, dt \qquad (4.9)$$

These are valid only for problems in which $\omega_n = n\omega_o$ with ω_o the fundamental frequency and n a positive integer. In all other cases, the limits on the integrals are $(t,\ t+2\pi/\omega_n)$.

The nonlinear coefficients A_{nij}, B_{nij} can be expressed (ref. 11) in terms of integrals over the mode shapes:

$$A_{nij} = \frac{1}{\bar{\gamma}E_n^2}\frac{1}{k_i^2 k_j^2}\{\tfrac{1}{2}(k_n^2+k_i^2+k_j^2)V_{nij} - \bar{\gamma}k_i^2 k_j^2 W_{nij}\} \qquad (4.10)$$

$$B_{nij} = -\frac{a^2}{\bar{\gamma}E_n^2}\{\tfrac{1}{2}(k_n^2 - \bar{\gamma}(k_i^2+k_j^2))V_{nij} + k_i k_j W_{nij}\} \qquad (4.11)$$

where

$$V_{nij} = \int \psi_n(\nabla\psi_i)\cdot(\nabla\psi_j)dV \ , \qquad (4.12)$$

$$W_{nij} = \int \psi_n\psi_i\psi_j dV \ . \qquad (4.13)$$

In the special case of ideal longitudinal modes when $\omega_n = n\omega_o$, the coefficients A_{nij} reduce to the special forms:

$$A_{nij} = \frac{V}{8\bar{\gamma}E_n^2 k_i^2 k_j^2}\left\{\left[(k_n^2+k_i^2+k_j^2)-2\bar{\gamma}k_i^2k_j^2\right]\delta_{n,|i-j|} - \left[(k_n^2+k_i^2+k_j^2)+2\bar{\gamma}k_ik_j\right]\delta_{n,i+j}\right\} \quad (4.14)$$

$$B_{nij} = -\frac{Va_o^2}{8\bar{\gamma}E_n^2}\left\{\left[k_n^2-\bar{\gamma}(k_i^2+k_j^2)+2k_ik_j\right]\delta_{n,|i-j|} + \left[k_n^2-\bar{\gamma}(k_i^2+k_j^2)-2k_ik_j\right]\delta_{n,i+j}\right\} \quad (4.15)$$

Equations (4.8) and (4.9) become first order nonlinear differential equations for the functions $A_n(t)$ and $B_n(t)$. The expression (4.7) is substituted in the integrals, and, owing to the relatively slow variations of $A_n(t)$, $B_n(t)$, the may be taken as essentially constant for the integration. With the formulas (4.14) and (4.15) taken into account, the differential equations can eventually be written

$$\frac{dA_n}{dt} = \alpha_n A_n + \theta_n B_n - \frac{n\beta}{2}\sum_{i=1}^{\infty}\left[A_i(A_{i-n}+A_{i+n}-A_{n-i}) + B_i(B_{i-n}+B_{i+n}+B_{n-i})\right] \quad (4.16)$$

$$\frac{dB_n}{dt} = \alpha_n B_n + \theta_n A_n + \frac{n\beta}{2}\left[A_i(B_{i-n}-B_{i+n}+B_{n-i}) - B_i(A_{i-n}-A_{i+n}-A_{n-i})\right] \quad (4.17)$$

The constants $\alpha_n = -D_{nn}/2$ and $\theta_n = -E_{nn}/2$ have been defined to simplify the forms.

Obviously, α_n is the growth or decay constant for the n^{th} harmonic: if all other terms on the right hand side are ignored, $A_n = \alpha_n A_n$, which has solution $A_n = A_n(0)\exp(\alpha_n t)$. Hence, the n^{th} harmonic grows exponentially in time, the familiar behavior for an unstable linear system. This shows that the nonlinear analysis reduces correctly to the case of linear motions, a feature which is essentially built in because of the way in which the analysis is constructed. It should be apparent that the approximate nonlinear analysis accommodates all linear results.

It is not possible to obtain formal solutions to equations (4.16) and (4.17), so completion of the approximate analysis requires numerical solutions. Because the oscillatory part of the motion has been removed, solutions can be obtained quite inexpensively: computation of one (or less) value of $A_n(t)$ and $B_n(t)$ per cycle is sufficient. However, it is necessary to truncate the expansions (4.1) and (4.2); the disturbance is approximated by a finite number of harmonics. This constitutes a rather serious approximation which requires further examination than will be given here.

The examples treated in the following will be based on expansion in five harmonics only. The numerical analysis does not yield information about the individual harmonics; because it is closely an "exact" solution, it contains essentially all harmonics. It will become apparent in what follows that truncation of the expansions is in some respects considerably more serious than in others. However, to the present time, the improvement achieved by accounting for more harmonics has not been examined. There is no difficulty in doing so; only a straightforward extension of the numerical routine is required to handle more simultaneous equations.

V. Summary Comparison of the Analyses

In order to contrast more clearly the analyses, it is useful to list the most important features and how they are treated. Only those differences which are built into the formulation are covered here. Other points will arise in the discussion of results.

Numerical Analysis	Approximate Analysis
steady-state solution:	
one-dimensional; calculated as part of the analysis.	uniform pressure, specified as part of the input.
gasdynamics:	
nonlinear, one-dimensional, exact; calculated by finite differences.	nonlinear, to second order, three-dimensional (one-dimensional here): expansion in harmonics; finite number of harmonics accounted for
surface combustion:	
transient, nonlinear or linear; quasi-steady gas phase; same physical model used in approximate analysis.	linear frequency response, short-time transients ignored.
influence of condensed material:	
nonlinear, transient behavior (exact).	linear, short-time transients ignored.
nozzle:	
quasi-steady, fractional lag analysis for two-phase flow.	quasi-steady; equilibrium two-phase flow.
results:	
transient behavior of any initial disturbance; usually, the time-dependent pressure, velocity and burning are printed and plotted.	primary output comprises the time-dependent amplitudes and phases of the harmonics: only initially sinusoidal disturbances have been treated.

It should be particularly noted that the transient behavior of combustion is a crucial part of the problem. While the same physical model for pressure coupling (essentially that reviewed in ref. 15) is used in both analyses, two additional simplifications are used in the approximate analysis. Only linear behavior is treated, and the burning is assumed to respond instantaneously to each harmonic of the pressure disturbance.

Both kinds of analyses will accommodate distributions of particle sizes, but the results covered here will be for a single particle size only.

VI. Development of Waves in a Box

This is the simplest kind of problem which can be treated. There is no combustion or flow; a

two-phase mixture of gas and particles is contained in a box enclosed by a rigid boundary. Initially, a disturbance is introduced having the form of the fundamental mode for the box. Thus, the unsteady pressure fluctuation has one or the other of the two forms for $t \to 0$:

$$\frac{p'}{p_o}(t \to 0) = \Delta p \cos\left(\frac{\pi z}{L}\right)\cos \omega t \qquad (6.1)$$

or

$$\frac{p'}{p_o}(t \to o) = \Delta p \cos\left(\frac{\pi z}{L}\right)\sin \omega t \ . \qquad (6.2)$$

In the first case, the velocity fluctuation is everywhere zero initially; and in the second case, the velocity fluctuation is non-zero, and the pressure fluctuation is zero. The first case is somewhat easier to handle in the numerical analysis because the velocities of the particles and gas are everywhere zero at $t = 0$.

Figures 1-5 show some waveforms computed by using the two analyses, for the cases of particle diameters ranging from zero (i.e., no particles present) to 100 microns. The ratio of the mass of condensed matter to the mass of gas is 0.36, and in all cases the frequency is 900 Hz. That the exact analysis is for a nonlinear drag law, and the approximate analysis is for a linear drag law must be taken into account when these results are examined. The exact analysis has not, to the present time, been performed for a linear drag law.

The case $\sigma = 0$ (no particles) shows most clearly that the approximate analysis involves only a small number (here, five) of harmonics. Figure 1 shows very obviously the generation of the harmonics due to nonlinear coupling. The exact solution exhibits the steepening one would expect on the leading edge of the wave, ultimately becoming too sharp to be accommodated accurately as the analysis is presently constructed. A peculiar difference appears in the approximate analysis between the two initial conditions, shown in Figure 2. The result for the condition (6.2) is in better agreement with the exact solution, for reasons not known at this time.

Figures 3-5, illustrating the influence of the dissipation of energy, for the most part exhibit the behavior one would expect. However, a few details were not anticipated. The curves for the pressure disturbances at the center of the box, and the curves labeled "even harmonics" for the approximate analysis, show the initial generation and eventual attenuation of higher even harmonics.

Ultimately, for small amplitudes, the attenuation coefficient $\alpha = \tau^{-1} \ln \delta p$, where τ is the period and δp is the difference in peak pressure for two successive maxima, approaches the value expected from linear analysis (eq. 7.3). For large amplitudes, the value of α is substantially different from the linear value, and depends both on the amplitude and on the previous history of the wave. The reason for this is that if the initial condition includes only the first harmonic, the amount of higher harmonics present depends on how long the wave has developed. Thus, for example, the value of α for a wave initially started with $\Delta p = .05$ is in the first cycle of decay, different from the value of α at the same amplitude for a wave which has decayed from, say, an initial amplitude of .2. Table 6.1 shows the values of α and the corresponding amplitudes for two cases of waves in a gas containing particles having diameter equal to 8 microns. The waveforms for these cases are shown in Figure 4. The rather large changes in attenuation coefficient with amplitude and between the exact and approximate solutions are not apparent from the waveforms themselves. The sharp, almost discontinuous, changes appearing in some of the approximate results are presently unexplained; they may be associated with limitations of the numerical routine used to solve the nonlinear differential equations.

As one should expect, the attenuation coefficient is not constant as the wave decays. For the approximate solution, the change in α is due to the

Fig. 1. Development of a Wave, No Particles; $\Delta p = 0, 1$ at $t = 0$.

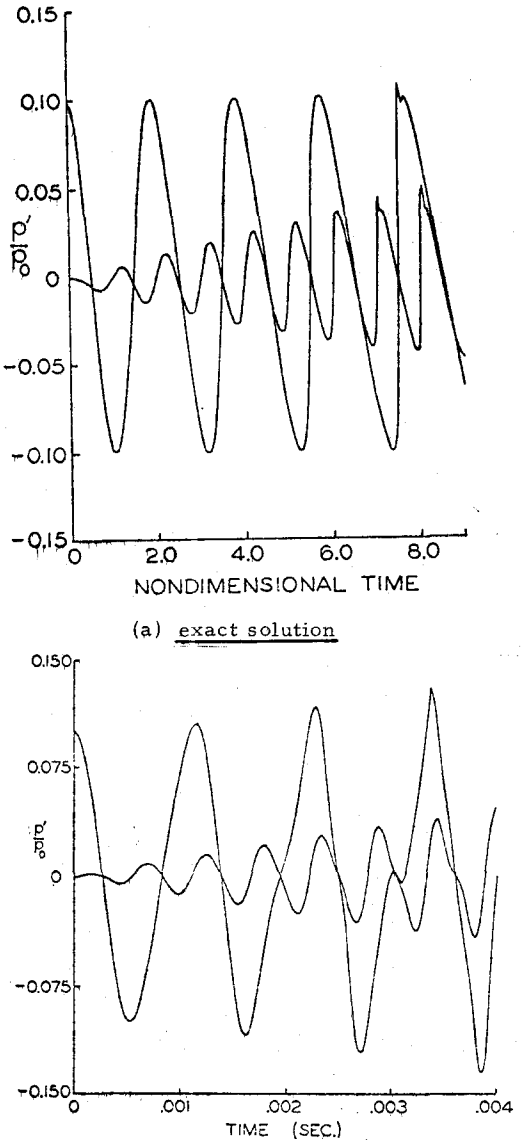

(a) exact solution

(b) approximate solution

Table 6.1 Calculated Attenuation Coefficients; Diameter of Particles Is 8 Microns (linear value: $\alpha = 582\ sec^{-1}$).

Initial Amplitude 5 per cent

Exact			Approximate		
Cycle	Amplitude	$\alpha\ (sec^{-1})$	Cycle	Amplitude	$\alpha\ (sec^{-1})$
1	.050 .030	402	1	.050 .025	578
2	.03 .018	430	2	.025 .012	591
3	.018 .011	450	3	.012 .0057	595
			4	.0057 .0030	503

Initial Amplitude 20 per cent

Exact			Approximate		
Cycle	Amplitude	$\alpha\ (sec^{-1})$	Cycle	Amplitude	$\alpha\ (sec^{-1})$
1	.200 .136	340	1	.200 .099	557
2	.136 .088	366	2	.099 .048	650
3	.088 .056	384	3	.048 .021	643
4	.056 .035	389	4	.021 .009	545

Figure 2. Development of a Wave, No Particles; Approximate Solution for Two Initial Conditions.

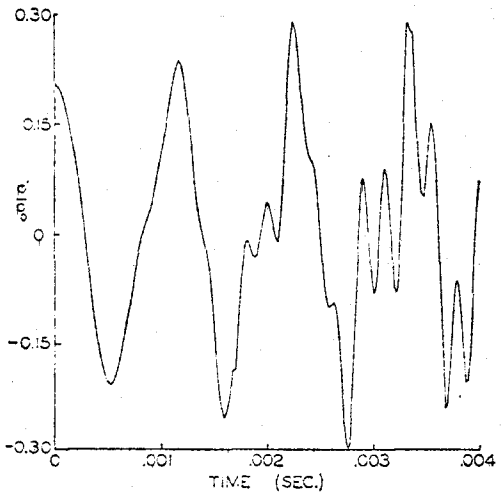

(a) initial condition (6.1) ($\Delta p = .2$ at $t = 0$)

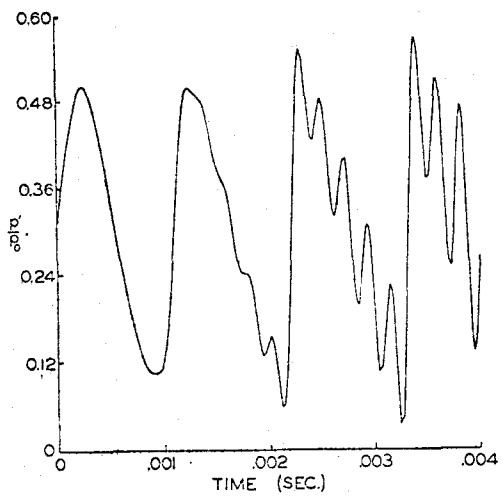

(b) initial condition (6.2) ($\Delta p = .2$ at $t = 0$)

nonlinear coupling between harmonics. In the exact solution, the nonlinear drag law also influences the behavior, but the limited results obtained so far do not allow one to separate the relative importance of the two nonlinear processes. Note particularly that for the exact solution, the level of α is smaller for larger amplitudes; the trend is reversed in the approximate solution.

It appears from the exact solution that tentatively one may offer the following generalizations. For both large and small particles, in the presence

Figure 3. Attenuation of a Wave, $\sigma = 3$ microns, $\Delta p = 0.2$ at $t = 0$.

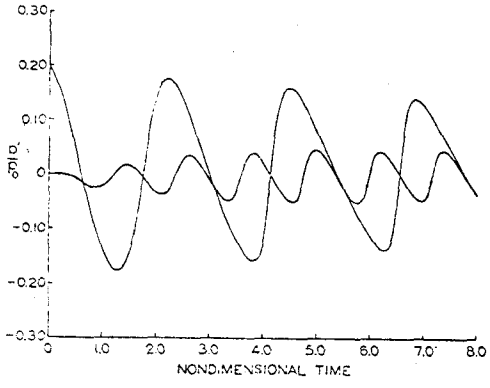

(a) exact solution

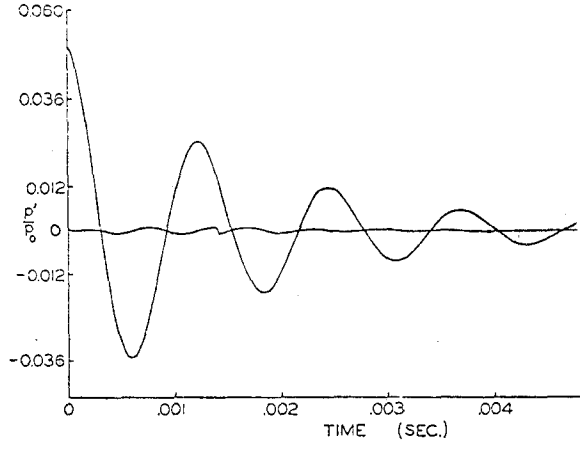

(b) $\Delta p = .05$ at $t = 0$; approximate solution

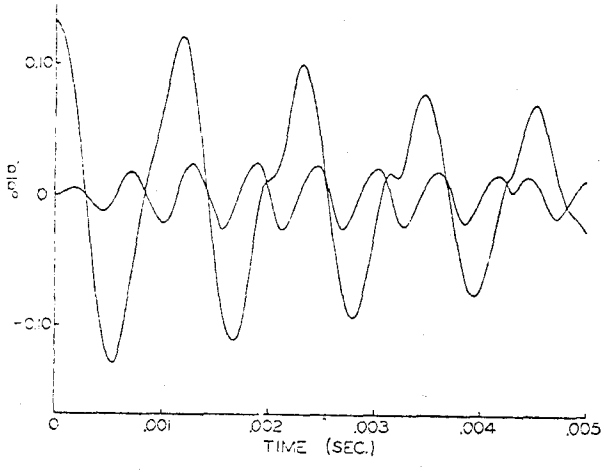

(b) approximate solution

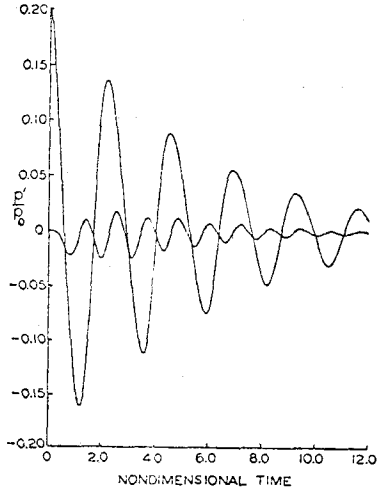

(c) $\Delta p = 0.2$ at $t = 0$; exact solution

Figure 4. Attenuation of a Wave, $\sigma = 8$ microns.

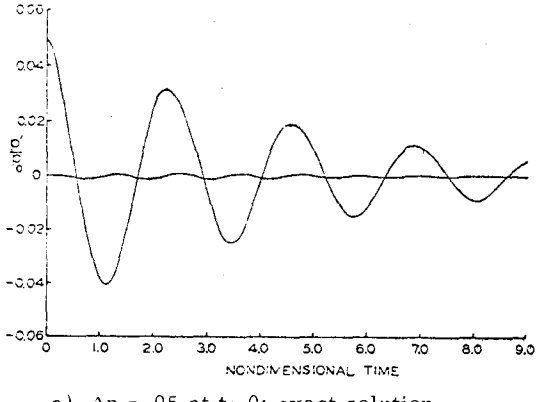

a) $\Delta p = .05$ at $t = 0$; exact solution

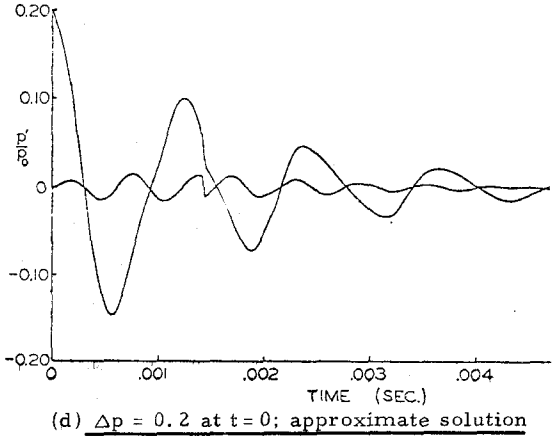

(d) $\Delta p = 0.2$ at $t = 0$; approximate solution

Figure 5. Attenuation of a Wave, $\sigma = 100$ microns, $\Delta p = .2$ at $t = 0$; exact solution.

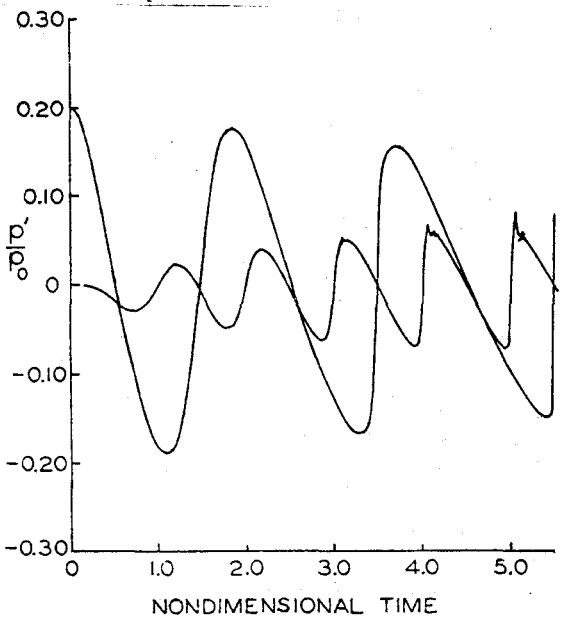

of an initially pure fundamental wave, the attenuation coefficient as a function of amplitude first increases with amplitude. It may then decrease slightly, but for large amplitudes increases monotonically with amplitude. For particles near the optimum size for a given frequency, the attenuation appears to decrease slightly with amplitude. It is not clear at this time just how much of this behavior should be attributed to the nonlinear drag law.

For the frequency (900 Hz) chosen for these calculations, the particle size for maximum linear attenuation is about 8 microns. The linear attenuation coefficients at this frequency are 143 sec^{-1}, 582 sec^{-1}, and 8.6 sec^{-1} for the 3, 8, and 100 micron particles, respectively. Smaller sizes more effectively attenuate the higher frequencies generated by the nonlinear gasdynamics. Comparison of Figures 3a, 4c, and 5 show this feature very clearly for the exact solution. Indeed, the largest (100 micron) particles so ineffectively damp the higher frequencies that the wave quite rapidly develops a very sharp front. The approximate analysis produces qualitatively the same behavior.

VII. Some Results for a Small Motor

The results covered in this section are part of some calculations performed to interpret a series of tests carried out several years ago (Ref. 18). In the following table, the data required for the approximate analysis are listed. Most are also required for the exact analysis; but in that case, the mean pressure, the response of the burning rate, and the speed of sound are computed as part of the solution.

Geometric Variables

length	$L = 0.5969$ m
port radius	$r_c = 0.0253$ m
throat area/port area	$J = 0.137$

Combustion Variables

linear burning rate	$\bar{r} = .00813\left(\frac{\bar{p}}{500}\right)^{.3}$ m/sec
parameters in the combustion response	$A = 6.0$ $B. = 0.55$
mean pressure	$p_o = 1568$ psia
chamber temperature	$T_c = 3540^{\circ}K$
mass particles/mass gas	$C_m = .36$
particle diameter	$\sigma = 2 \times 10^{-6}$ m

Physical Properties

Prandtl number	$Pr = .8$
thermal diffusivity of propellant	$\kappa = 0.001$ cm^2/sec
specific heat of gas	$C_p = 2020$ Joule/kgm-$^{\circ}K$
specific heat of condensed material	$C_s = .68\ C$
coefficient of viscosity	$\mu = 0.8834\times10^{-4}\left(\frac{T_c}{3485}\right)^{.66}$
density of particle material	$\rho_s = 4.0$ gm/cm^3
density of gas	$\bar{\rho}_g = 9.15\left(\frac{p_o}{1500}\right)\left(\frac{T_c}{3370}\right)$
γ (gas only)	$\gamma = 1.23$
$\bar{\gamma}$ (mixture)	$\bar{\gamma} = \frac{\gamma(1+C_m C_s/C_p)}{(1+C_m\gamma\, C_s/C_p)}$
gas constant	$R = (\gamma-1)C_p/\gamma$
speed of sound in gas/particle mixture	$a_o = [\bar{\gamma}RT_c/(1+C_m)]^{\frac{1}{2}}$

7.1 Contributions to the Linear Growth Rate (Approximate Analysis)

Four contributions to linear stability are included in the approximate analysis; they arise from the nozzle, condensed material in the gas phase, inelastic acceleration of the flow leaving the burning surface, and the driving due to combustion. The formulas for the corresponding growth coefficients ($\alpha > 0$ for driving) are:

$$\alpha_{nozzle} = -a_o\left(\frac{J}{L}\right)\left(\frac{2}{1+\bar{\gamma}}\right)^{\frac{\bar{\gamma}}{2(\bar{\gamma}-1)}} \qquad (7.1)$$

$$\alpha_{flow} = -(1+C_m)\bar{u}_b/r_c \qquad (7.2)$$

$$\alpha_{particles} = -C_m\left\{\frac{\omega^2\tau_d}{1+(\omega\tau_d)^2} + (\gamma-1)\frac{C_s}{C_p}\frac{\omega^2\tau_t}{1+(\omega\tau_t)^2}\right\} \qquad (7.3)$$

$$\alpha_{combustion} = \frac{\bar{\gamma}\bar{u}_b}{r_c}(1+C_m)R_b^{(r)} \qquad (7.4)$$

where $\bar{u}_b$ is the average speed of the material leaving the burning surface, $\tau_t = 3(C_s Pr/C_p)\tau_d$ and τ_d is the relaxation time for the particle motion,

$$\tau_d = \rho_s\sigma^2/18\mu\ . \qquad (7.5)$$

The formula (7.3) used for the attenuation by the particle/gas motions may be found in ref. 19; it may also be found directly by using the linear stability analysis discussed in refs. 4 and 5. The loss due to flow turning has been discussed in ref. 4.

Because there are time lags associated with the motion of the particles and the response of the burning surface, those processes also contribute to the quantity θ defined in § 4:

$$\theta_{\text{particles}} = -\alpha_{\text{particles}} , \qquad (7.6)$$

$$\theta_{\text{combustion}} = -\frac{R_b^{(i)}}{R_b^{(r)}}\,\alpha_{\text{combustion}} . \qquad (7.7)$$

Note that the frequency Ω depends on the harmonic, so while (7.1) and (7.2) have the same values for all harmonics, (7.3)-(7.7) do not.

The real part $R_b^{(r)}$ of the response function for A = 6 and B = .55 and .56 is plotted in Figure 6. It happens that in this range of parameters, the response is very sensitive to the value of B. In Figure 7, the values of α and θ for the first five harmonics are shown. The vertical line is drawn at 900 Hz to emphasize the values associated with an example given below. Note that only the first harmonic is unstable (i.e., $\alpha_1 > 0$) at this frequency.

Figure 6. The Real Part of the Linear Harmonic Response Function for A = 6.0 and B = 0.55, 0.56.

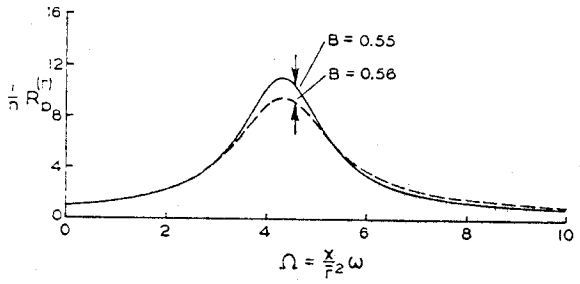

Figure 7. Linear Coefficients for Five Harmonics.

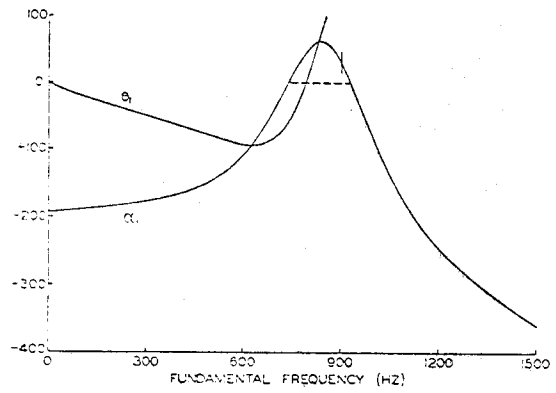

(a) first harmonic

8.2 Computation of an Unstable Disturbance

The driving for an unstable motion derives from the interactions between the pressure disturbance and the burning processes. According to linear theory, it is the real part of the response function which mainly contributes. For the data and formulas given above, the linear growth constants for A = 6 are $\alpha_1 = 8.68\ \text{sec}^{-1}$ when B = .55 and $\alpha_1 = -9.5\ \text{sec}^{-1}$. The difference, causing a small disturbance to be unstable for B = .55 and stable for B = .56, is due solely to the change in the response function, shown in Figure 6.

Figure 7. Linear Coefficients (continued).

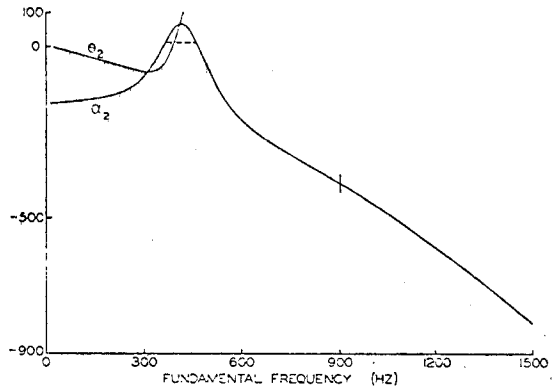

(b) second harmonic

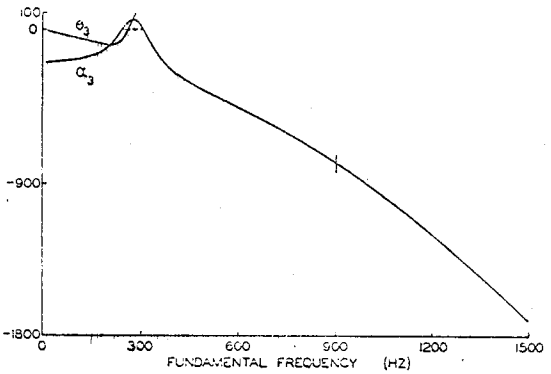

(c) third harmonic

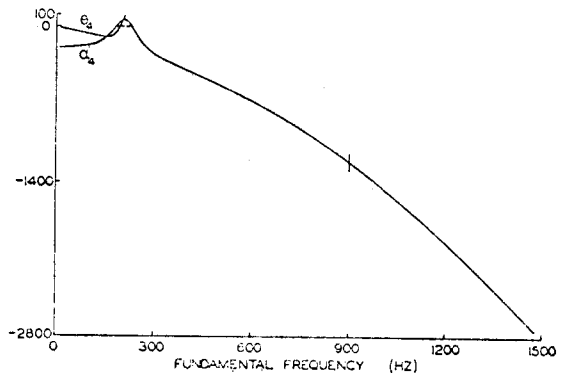

(d) fourth harmonic

Both the exact and approximate analyses show stability for B = .56 and instability for B = .55 when A = .55. Because the exact analysis incorporates a nonlinear calculation of the burning response, unique values if A and B cannot be assigned, except for infinitesimally small amplitudes. However, the conclusion concerning stability is valid.

Figure 7. Linear Coefficients (continued).

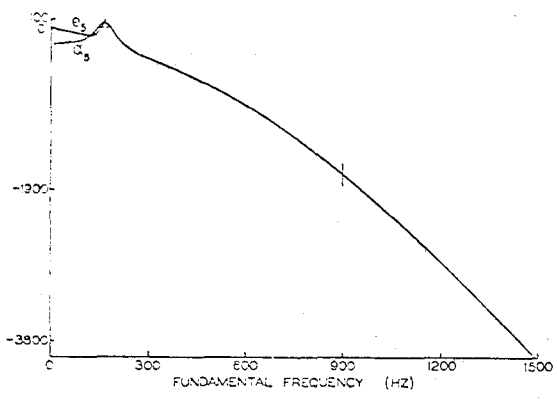

(e) fifth harmonic

Calculated results are shown in Figures 8 and 9 for an initial disturbance having the form of the fundamental mode with an amplitude of 5 per cent of the mean pressure. The limiting amplitudes reached are considerably different -- approximately 4.2 per cent for the exact analysis and 4.9 per cent for the approximate analysis. In Figure 9, the history of the amplitudes for the five harmonics is shown.

Figure 8. Transient Waveforms for an Unstable Disturbance.

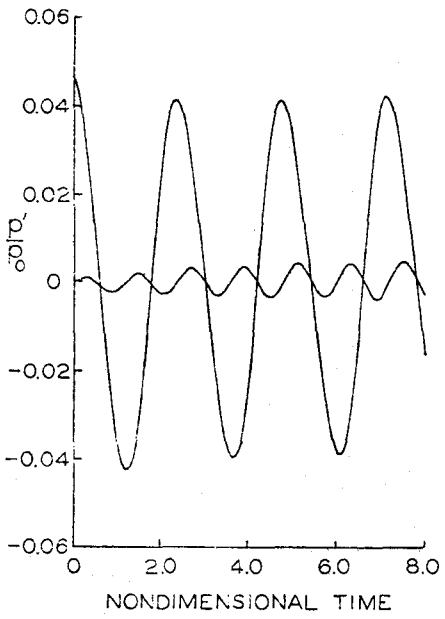

(a) exact solution

It is not possible at this time to state definitely which process accounts for the difference -- possibly, of course, all do. The approximate analysis demonstrates that the gasdynamic nonlinearity alone serves to limit the amplitudes at reasonable values. Moreover, even with only five harmonics accounted for, the waveform does not appear greatly different from that computed with the exact

Figure 8. Transient Waveforms (continued).

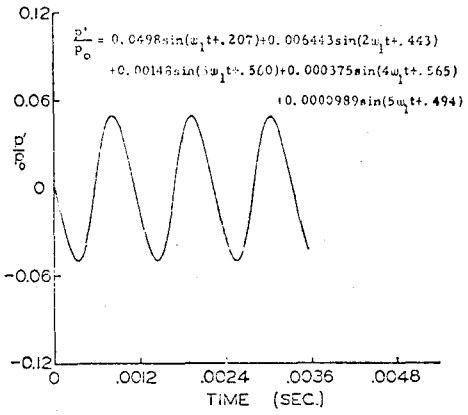

(b) final waveform, approximate solution

analysis (Figure 8). This is a striking and very encouraging result.

Figure 9. Growth of the Amplitudes of the First Five Harmonics.

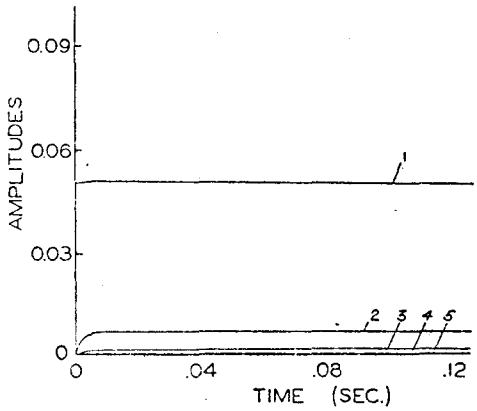

The nonlinear behavior of the burning rate probably has little influence on the limiting oscillations. Figure 10 shows the fluctuations of pressure and burning rate for two calculations using the exact analysis: in one the linear representation is used, and in the other the response was calculated using the nonlinear differential equations. The values of A and B are different, but otherwise all numerical values are identical to those listed above. While the unsteady burning rate is obviously different for the two cases, the pressure wave in the chamber appears essentially the same. Moreover, the average burning rate is essentially the same for the two cases.

Consequently, one is inclined at present to ascribe the difference shown in Figure 8 to the nonlinear behavior of the particles, nozzle, or gasdynamics. The first two are included as linear processes in the approximate analysis, and the last has been treated only to second order. The results of § 6 suggest that the nonlinear behavior of particle motions may indeed be very significant to the detailed behavior of the acoustic waves. In later work, both this and a better approximation to the nonlinear acoustics will be examined within

the framework described in § 4. No statement can be made concerning the influence of nonlinear behavior of the nozzle. This is much more difficult to incorporate in the approximate analysis.

Figure 10. Comparison of Linear and Nonlinear Burning Rates (Exact Solution).

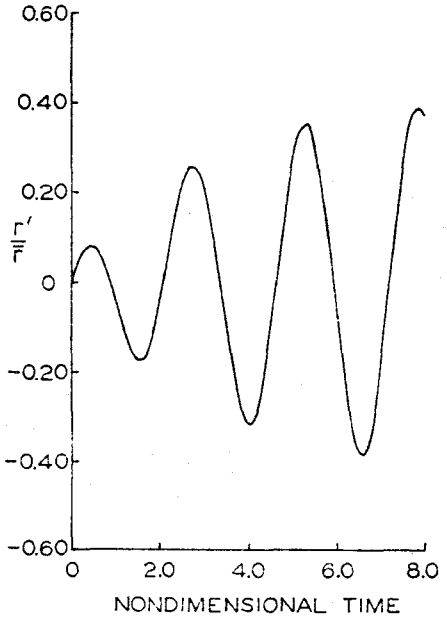

a) Linear burning rate (A = 5, B = .48)

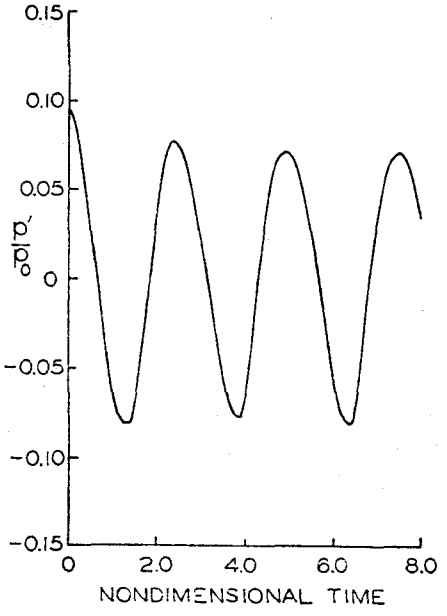

b) Pressure wave for the burning rate of a)

VIII. Concluding Remarks

The results of both the exact and approximate analyses are very encouraging. It must be emphasized that the exact numerical analysis serves two primary purposes: as a means of interpreting data such as those made available to the authors by

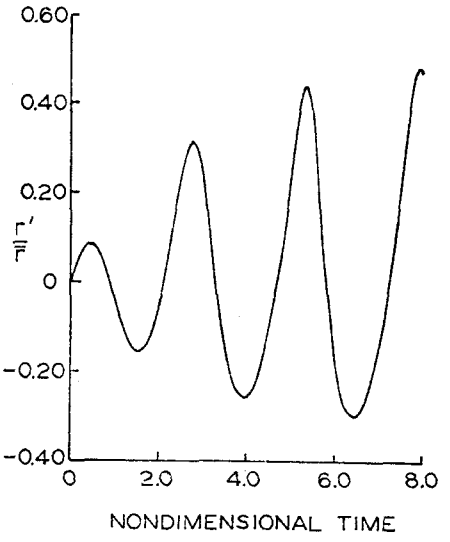

c) Nonlinear burning rate (A = 5, B = .48)

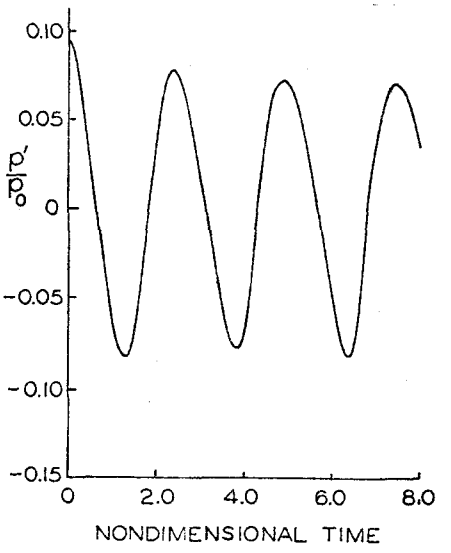

d) Pressure wave for the burning rate of c)

ref. 18, and as a check of approximate analyses such as that discussed in the present work. Both analyses seem to agree very well in the linear limit; the present results, together with others not reported here, indicate that with realistic values of all input parameters (including those appearing in the combustion response) the stability of the disturbances is computed to be at least in qualitative agreement with the observations of ref. 18. There are, however, difficulties and uncertainties in predicting trends with mean pressure .

It is particularly to be noted (1) that the value of the response function (3. 1 for the result shown in Figures 8 and 9) is, as far as presently is known, a reasonable value; and (2) that the limiting amplitudes also appear to be in fairly good

agreement with observed values.

In a somewhat more general vein, the results presented in this work justify the following observations:

1) The substantial difference in the behavior of the approximate solution with a change of initial condition (Figure 2) suggests that the expansion of the original differential equations should be carried out to third order if amplitudes larger than 10 per cent (roughly) are to be treated.

2) The results shown in Figure 10 imply that for amplitudes roughly less than 10 per cent (and perhaps larger as well - the limit has not been established) it is sufficiently accurate to use a linear representation of the combustion response.

3) The comparison of the exact and approximate results for the attenuation of waves by gas/particle interactions demonstrates that for transient motions, even when small amplitudes are reached, a nonlinear drag law should be used. The combined influences of the nonlinear generation of harmonics and the dependence of attenuation (by particle/gas interactions) on frequency are very important during the first few cycles of transient decay.

4) With the approximate analysis, fairly reasonable results are obtained even when the only nonlinear process is gasdynamics. But undoubtedly better values for the limiting amplitude will be found when nonlinear gas/particle interactions are accounted for. For very large amplitudes - the lower bound has not been found - it will be necessary to use a nonlinear representation of the combustion response.

Perhaps the most important general conclusion is that the limiting amplitude of many observed instabilities in motors is undoubtedly dominated by gasdynamic nonlinearities, with nonlinear gas/particle interactions providing a further reduction. This implies that for a given propellant, essentially the only practical means of affecting the limiting amplitude must involve changes of geometry, including, perhaps, the use of suppression devices.

Obviously, one cannot claim to be in a position to compute from first principles the transient nonlinear behavior of disturbances in a rocket motor. Many of the required physical quantities are not known accurately -- for example, the sizes of particles in the flow, and most of the parameters appearing in the respresentation of the combustion response. However, the success which has been achieved is significant, especially compared with the very meager knowledge available several years ago. The usefulness of an elaborate numerical analysis has been demonstrated, not only for increasing one's understanding of the processes involved in a motor, but also as a means of checking an approximate analysis.

It is unlikely that a complete numerical analysis will soon prove useful for studying three-dimensional motions. In principle, such problems can be solved numerically, but at great expense. The approximate analysis can be used, not as cheaply and easily as for one-dimensional problems, but the increased effort is not at all unreasonable. Hence, it is important to establish the validity of the approximations. This can only be done by the sorts of computations reported here.

Acknowledgment

This work was supported partly by the National Aeronautics and Space Administration under the Jet Propulsion Laboratory Contract NAS 7-100; and partly by the Air Force Rocket Propulsion Laboratory under Contract No. F04611-71-C-0060.

REFERENCES

1. McClure, F. T., Hart, R. W., and Bird, J. F. "Solid Propellant Rocket Motors as Acoustic Oscillators," Progress in Astronautics and Rocketry, V. 1, Academic Press, New York (1960), pp. 295-358.

2. Cantrell, R. H. and Hart, R. W., "Interaction Between Sound and Flow in Acoustic Cavities: Mass, Momentum and Energy Considerations," J. Acoust. Soc. Amer., V. 36, no. 4 (April 1964), pp. 697-706.

3. Culick, F. E. C. "Acoustic Oscillations in Solid Propellant Rocket Chambers," Astronautica Acta, V. 12, no. 2 (Feb. 1966), pp. 113-126.

4. Culick, F. E. C. "Stability of One-Dimensional Motions in a Rocket Motor," Combustion Science and Technology, V. 7, no. 4 (1973), pp. 165-175.

5. Culick, F. E. C. "Stability of Three-Dimensional Motions in a Combustion Chamber," (submitted for publication).

6. Levine, J. N. and Culick, F. E. C. "Numerical Analysis of Nonlinear Longitudinal Combustion Instability in Metallized Propellant Solid Rocket Motors," 9th JANNAF Combustion Meeting (Sept. 1972), C. P. I. A. Pub. 231.

7. Levine, J. N. and Culick, F. E. C. "Nonlinear Longitudinal Combustion Instability in Solid Rocket Motors," 10th JANNAF Combustion Meeting (Aug. 1973).

8. Kooker, D. E. and Zinn, B. T. "Numerical Solution of Axial Instabilities in Solid Propellant Rocket Motors," 10th JANNAF Combustion Meeting (Aug. 1973).

9. Kooker, D. E. and Zinn, B. T. "Triggering Axial Instabilities in Solid Rockets: Numerical Predictions," AIAA/SAE 9th Propulsion Joint Specialist Conference, Las Vegas, Nevada (Nov. 1973), AIAA Paper No. 73-1298.

10. Culick, F. E. C. "Nonlinear Growth and Limiting Amplitude of Acoustic Waves in Combustion Chambers," Combustion Science and Technology, V. 3, no. 1 (April 1971), pp. 1-16.

11. Culick, F. E. C. "Nonlinear Behavior of Acoustic Waves in Combustion Chambers," 10th JANNAF Combustion Meeting (Aug. 1973).

12. Rudinger, G. "Effective Drag Coefficients for Gas-Particle Flow in Shock Tubes," Squid Technical Report CAL-97-PU (Mar. 1969).

13. Carlson, D. J. and Hoglund, R. F. "Particle Drag and Heat Transfer in Rocket Nozzles," AIAA J., V. 2, no. 11 (Nov. 1964), pp. 1980-1984.

14. Kliegel, J. R. "Gas-Particle Nozzle Flows," 9th (International) Symposium on Combustion, The Combustion Institute, Pittsburgh, Pa. (1963), pp. 811-826.

15. Culick, F. E. C. "A Review of Calculations for Unsteady Burning of a Solid Propellant," AIAA J., V. 6, no. 12 (Dec. 1968), pp. 2241-2254.

16. Kevorkian, J. "The Two-Variable Expansion Procedure for the Approximate Solution of Certain Nonlinear Differential Equations," Lectures in Applied Mathematics, V. 7, Space Mathematics, Part III, American Mathematical Society (1966), pp. 206-275.

17. Bogoliubov, N. N. and Mitropolskiy, Yu. A. Asymptotic Methods in the Theory of Nonlinear Oscillations, Hindustan Publishing Corp., Delhi (1961).

18. Micheli, P. L., Aerojet General Solid Propulsion Company (private communication).

19. Temkin, S. and Dobbins, R. A. "Attenuation and Dispersion of Sound by Particulate Relaxation Processes," J. Acoust. Soc. Amer., V. 40, no. 2 (Feb. 1966), pp. 317-324.